Journal of Biotechnology 173 (2014) 10–18

Contents lists available at ScienceDirect

Journal of Biotechnology

journal homepage: www.elsevier.com/locate/jbiotec

Development of a non-viral gene delivery vector based on the dynein light chain Rp3 and the TAT peptide

M.T.P. Favaro[a], M.A.S. de Toledo[a], R.F. Alves[b], C.A. Santos[a], L.L. Beloti[a], R. Janissen[c], L.G. de la Torre[d], A.P. Souza[a], A.R. Azzoni[b,*]

[a] Laboratório de Análise Genética e Molecular, Centro de Biologia Molecular e Engenharia Genética, Universidade Estadual de Campinas, Campinas, SP, Brazil
[b] Departamento de Engenharia Química, Escola Politécnica, Universidade de São Paulo, São Paulo, SP, Brazil
[c] Instituto de Física Aplicada "Gleb Wataghin", Universidade Estadual de Campinas, Campinas, SP, Brazil
[d] Faculdade de Engenharia Química, Universidade Estadual de Campinas, Campinas, SP, Brazil

ARTICLE INFO

Article history:
Received 16 October 2013
Received in revised form
20 December 2013
Accepted 2 January 2014
Available online 11 January 2014

Keywords:
Gene delivery
Non-viral protein vectors
Dynein light chain Rp3
TAT

ABSTRACT

Gene therapy and DNA vaccination trials are limited by the lack of gene delivery vectors that combine efficiency and safety. Hence, the development of modular recombinant proteins able to mimic mechanisms used by viruses for intracellular trafficking and nuclear delivery is an important strategy. We designed a modular protein (named T-Rp3) composed of the recombinant human dynein light chain Rp3 fused to an N-terminal DNA-binding domain and a C-terminal membrane active peptide, TAT. The T-Rp3 protein was successfully expressed in *Escherichia coli* and interacted with the dynein intermediate chain *in vitro*. It was also proven to efficiently interact and condense plasmid DNA, forming a stable, small (~100 nm) and positively charged (+28.6 mV) complex. Transfection of HeLa cells using T-Rp3 revealed that the vector is highly dependent on microtubule polarization, being 400 times more efficient than protamine, and only 13 times less efficient than Lipofectamine 2000™, but with a lower cytotoxicity. Confocal laser scanning microcopy studies revealed perinuclear accumulation of the vector, most likely as a result of transport *via* microtubules. This study contributes to the development of more efficient and less cytotoxic proteins for non-viral gene delivery.

1. Introduction

Gene therapy can be defined as the introduction of nucleic acids into cells with the goal of altering gene expression to prevent, halt or reverse a pathological process (Kay, 2011). Despite the great potential of these new therapies, gene therapy still faces major challenges because DNA requires a vector to protect and to transport it into the cell. An ideal vector should be safe, efficient and stable. However, finding such a vector remains a major challenge (Ganta et al., 2008; Ruponen et al., 2009). Viral vectors, biological carriers that have naturally evolved to transfer genetic materials into host cells (Lv et al., 2006), are efficient, although they are associated with several adverse effects ranging from inflammation to death, raising doubts about their safety (Edelstein et al., 2007; Vázquez et al., 2008). Non-viral vectors are less efficient but are considered to be safer, are cheaper to produce and have no limitations on the size of the DNA sequence delivered (Kay, 2011).

DNA delivery systems must overcome multiple extra- and intracellular barriers before reaching the nucleus. These barriers include binding to the cell surface, cell entry/endocytosis, endosomal escape, evasion of cytosolic nucleases and nuclear entry (Azzoni et al., 2007; Medina-Kauwe et al., 2005; Ruponen et al., 2009). One important obstacle that is often neglected in strategies that mimic viral trafficking is transport throughout the cytoplasm. Plasmid DNA cannot depend solely on diffusion during trafficking to the nucleus. Microinjection studies have demonstrated that naked pDNA larger than 2000 bp diffuses poorly if at all in the cytoplasm (Douglas, 2004; Lukacs et al., 2000; Suh et al., 2003). Additionally, free pDNA in the cytosol is rapidly degraded by endonucleases (Mastrobattista et al., 2006). Therefore, it has been suggested that dyneins may serve to improve the transport of pDNA toward the minus-end of microtubules (MT), which are usually located close to the cell nucleus (Döhner et al., 2005; Mesika et al., 2005; Moseley et al., 2010; Tzfira, 2006). Dynein is a multi-subunit protein complex formed by two dynein heavy chains (HC; ~530 kDa, responsible for ATP hydrolysis and binding to microtubules), two dynein intermediate chains (IC; ~74 kDa),

* Corresponding author at: Departamento de Engenharia Química, Escola Politécnica, Universidade de São Paulo, Av. Prof. Luciano Gualberto, Trav. 3, Nº 380, CEP 05508-900, São Paulo, SP, Brazil. Tel.: +55 11 30912234; fax: +55 11 30912284.
E-mail addresses: adriano.azzoni@poli.usp.br, adrianoazzoni@hotmail.com (A.R. Azzoni).

0168-1656/$ – see front matter © 2014 Elsevier B.V. All rights reserved.
http://dx.doi.org/10.1016/j.jbiotec.2014.01.001

several dynein light intermediate chains (LIC; ~52–61 kDa) and a number of dynein light chains (LC; ~10–25 kDa). The dynein light chains are from the LC8, TcTex/Rp3 and LC7/roadblock families and are responsible for cargo binding and the regulation of motor activity (Döhner et al., 2005; Holzbaur and Vallee, 1994).

Many viruses exploit microtubules *via* dynein motors to translocate to the nuclear periphery. For example, the herpes simplex virus type 1 binds to the dynein light chains Rp3 and TcTex1 to reach the nucleus (Dodding and Way, 2011; Douglas, 2004; Medina-Kauwe et al., 2005). The relevance of the microtubule network to the transport of pDNA complexes has been demonstrated (Suh et al., 2003), and the protein p53 also exploits this machinery to accumulate in the nucleus (Lo, 2004). Recently, Moseley et al. (2010) demonstrated that dynein light chain association sequences enhance the nuclear accumulation of exogenous proteins by exploring the MT network.

Our group recently demonstrated that the dynein light chain LC8 can be modified by inserting a synthetic DNA-binding motif while still maintaining the ability to interact *in vitro* with the dynein intermediate chain (Ferrer-Miralles et al., 2008; Toledo et al., 2012), forming positive particles that efficiently transfect HeLa cells *in vitro*. This process is dependent on MT transport and is minimally cytotoxic. We have also characterized the human dynein light chain Rp3 and shown that the simple addition of a DNA binding sequence transforms this dynein light chain into a promising gene delivery vector (Toledo et al., 2013). The human Rp3 has a molecular mass of approximately 13 kDa and is a member of the Tctex dynein light chain family. It exists in homodimeric and heterodimeric forms and is associated with Tctex1, although the heterodimer form is unable to bind to the dynein intermediate chain (King, 2000).

Here, recombinant Rp3 was fused to a N-terminal DNA binding domain and to the C-terminal TAT sequence, a cell penetrating peptide (CPP) (Azzoni et al., 2007; Won et al., 2011), to form a novel protein named T-Rp3. Cell penetrating peptides are also known as protein transduction domains (PTDs) and are usually short peptides that are rich in basic amino acids (Said Hassane et al., 2009). These peptides originate from proteins that are naturally capable of crossing membranes and have been used to study the delivery of bioactive molecules, including nucleic acids (Yamano et al., 2011). The better-known CPP is represented by TAT, an arginine-rich peptide derived from HIV-1 trans-activator protein (Won et al., 2011). The mechanism of TAT entry into the cell is the subject of some debate, but entry has been shown to be concentration and cell type-dependent (Ferrer-Miralles et al., 2008; Gump and Dowdy, 2007; Moschos et al., 2007). TAT is also promising for gene delivery because it has an additional ability of entering the cell nucleus with much faster kinetics than nuclear import mediated by the nuclear localization signal (NLS) (Nitin et al., 2009). In resume, this work presents a step forward on the development of modular proteins for non-viral gene delivery based on dynein light chains. Besides the inclusion of a new domain on the Rp3 protein, the TAT cell penetrating peptide, we could better characterize and evaluate the pDNA–protein complexes, transfection efficiency and cellular uptake of the non-viral particles, adding new information to the development of non-viral gene delivery vectors based on modular proteins.

2. Materials and methods

2.1. Plasmid DNA vector

The plasmid DNA used in this study was previously described by Toledo et al. (2012). Named pVAX1-Luc, the plasmid was constructed by replacing the GFP-encoding sequence of the pVAX1-GFP plasmid (Azzoni et al., 2007) with the luciferase gene sequence obtained from the pGL3-Luc control vector (Promega). Purification of the pVAX1-Luc plasmid used in all transfection studies was performed as described by Freitas et al. (2007).

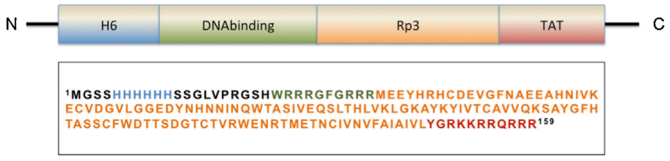

Fig. 1. The T-Rp3 recombinant protein. Illustrative distribution of functional modules in T-Rp3 and the amino acid sequence of the protein construct, which contains a histidine tail (H6 – in blue), the synthetic DNA-binding sequence (green), the Rp3 human dynein light chain (orange), and the TAT sequence (red). The residues resulting from the cloning process are shown in black. (For interpretation of the references to color in this figure legend, the reader is referred to the web version of the article.)

2.2. Recombinant protein expression and purification

The TAT DNA sequence was cloned into the pET28a expression vector (Merck). The TAT sequence was synthesized as two complementary single oligonucleotide strands containing the amino acid sequence YGRKKRRQRRR (Nitin et al., 2009) optimized for expression in *Escherichia coli*. The complementary sequences were annealed and phosphorylated prior to cloning in pET28a, which was previously digested with *Eco*RI and *Xho*I. The vectors were then transformed into *E. coli* strains.

The fusion protein DNA-binding domain WRRRGFGRRR (named DNAb4) was previously designed by Toledo et al. (2012) for peptide and protein domains with high DNA binding and condensing capacity. The DNAb4 domain was fused to the Rp3 sequence amplified from HeLa cell cDNA as described previously (Toledo et al., 2012). The Rp3 protein sequence containing the DNA-binding sequence was amplified and inserted in the pET28a plasmid encoding the TAT sequence described above using specific primers (forward: 5′-GATAATGCTAGCTGGCGTCGCCGTGGTTTTG-3′ and reverse: 5′-GCAAGCCTTAAGAAGAACAATAGCAATGGCAA-3′). The fragment was cloned into the pET28a vector (Merck) using the *Nhe*I and *Eco*RI restriction sites. The resulting fusion protein (DNAb4-Rp3-TAT) is named T-Rp3 (Fig. 1).

The recombinant T-Rp3 was expressed in *E. coli* BL21 (DE3). Briefly, cells were grown in 1 L of LB media at 37 °C with shaking at 300 rpm until an optical density of 0.8 AU was reached (measured at 600 nm). Protein expression was induced with 5.6 mM lactose for an additional 20 h at 28 °C and shaking at 200 rpm. After centrifugation, the cell pellet was resuspended in 50 mM Tris (pH 7.0), 1 M NaCl, 0.1 mM EDTA, 15 mM β-mercaptoethanol and 1 mM PMSF (phenylmethylsulfonyl fluoride). Cell lysis was achieved by sonication and the lysate was clarified by centrifugation (12,000 × *g* for 20 min). The T-Rp3 in the clarified lysate was purified by a single Ni-NTA affinity chromatography step and eluted using an imidazole gradient in suspension buffer. The protein was then dialyzed in 40 mM HEPES buffer (pH 7.3), a condition that favored protein stability.

2.3. In vitro interaction of T-Rp3 with the dynein intermediate chain

To assess the interaction of the recombinant T-Rp3 with the dynein complex, we expressed and purified the N-terminus (first 300 amino acids) of the human dynein intermediate chain DYNIC2, isoform C, according to the protocol described by Toledo et al. (2012). The purified protein was subsequently immobilized in CNBr-activated Sepharose resin (GE Healthcare) following the manufacturer's protocol. The resin was packed into a 1-mL gravity column (Bio-rad). The protein solution loaded onto the resin

was composed of an equimolar mixture of T-Rp3 and Lc8 in 40 mM HEPES buffer (pH 7.3). The Lc8 intermediate chain was produced as previously described (Toledo et al., 2012). The inclusion of Lc8 was based on the premise that the presence of one light chain enhances the affinity of a second light chain to the dynein intermediate chain (Makokha et al., 2002; Hall et al., 2009). The washing step was conducted using adsorption buffer and elution was performed with an increasing concentration of salt (0.1, 0.5 and 1.0 M NaCl). A final desorption step was performed at pH 3.0. The pH of the latter elution fractions was immediately raised using Tris buffer (pH 9.0). Finally, the protein profiles of the collected fractions were analyzed by SDS-PAGE.

2.4. Evaluation of pDNA–protein interaction by gel retardation assay

To evaluate the ability of T-Rp3 and protamine to interact and condense pDNA, we performed a gel retardation assay. Proteins were dialyzed in 40 mM HEPES (pH 7.3) and incubated with 1 μg of pVAX1-Luc vector (previously in PBS) at different pDNA:protein molar ratios (1:100, 1:200, 1:500, 1:1000, 1:4000 and 1:8000) in a final volume of 50 μL. Protamine sulfate powder was resuspended in PBS. The samples were incubated at room temperature for 1 h, followed by the addition of 50 μL of non-supplemented F-12 media and an additional incubation for 20 min. Samples were run on a 0.8% agarose gel and visualized by ethidium bromide staining.

2.5. Zeta potential and dynamic light scattering assays

Zeta potential measurements were performed to comparatively evaluate the surface charge of complexes formed by pDNA:T-Rp3 at different molar ratios. Complexes were formed as previously described for the gel retardation assay, but without adding F-12 media. Each sample was measured six times using the Malvern Zetasizer Nano ZS (Malvern). The average hydrodynamic diameter and size distribution (number-weighted) of the complexes were measured *via* the dynamic light scattering (DLS) as described by Toledo et al. (2012). The pDNA:T-Rp3 complexes were measured at a molar ratio of 1:8000. Complexes were formed with 1 μg of pDNA and the corresponding amount of protein in a final volume of 800 μL. Each sample was subjected to multiple readings in a 60-min period.

2.6. Culture and transfection of HeLa cells

HeLa cells were grown in a F-12 (Ham) nutrient mixture (Gibco) containing 10% (v/v) fetal bovine serum (growth medium, Gibco). The cells were cultured in 75 cm^2 culture flasks and incubated in a 5% CO_2 humidified environment at 37 °C. Following growth to confluence, cells were trypsinized and seeded in 24-well culture plates (5×10^4 cells per well). The cells were incubated for 48 h (to 70% confluence) and then transfected with pDNA:protein complexes formed as described previously for gel retardation assays, using the same molar ratios. When indicated, transfection was carried out using the Lipofectamine 2000™ reagent (Invitrogen) according to the manufacturer's instructions (1 μg pDNA plus 1.5 μL reagent in 100 μL of medium per well) or protamine sulfate (Sigma–Aldrich, Germany). All transfections were carried out in the presence of serum. The medium containing the transfection solution remained on the transfected cells for 6 h and was then replaced with fresh growth medium. Cells were collected 24 h post-transfection and luciferase activity was determined by utilizing the Luciferase Assay System (Promega) according to the manufacturer's instructions. Luminescence intensity was normalized against the protein concentration in each transfection sample, determined by the Micro BCA Protein Assay Kit (Thermo Scientific). We used Lipofectamine 2000™ as a control because it is regarded as an effective and fast-acting transfection agent. The transfection assays were performed as three independent replicates (experiments performed independently), except using protamine (eight independent replicates), T-Rp3 (twelve independent replicates) and Lipofectamine 2000™ (six independent replicates).

To evaluate the contribution of the microtubule network in the intracellular trafficking of the complexes, cells were pre-incubated for 2 h with nocodazole (25 μM) (Sigma–Aldrich) to disrupt the microtubules. The drug was dissolved in DMSO and an equal volume of drug-free DMSO (0.4%) was used as a control. Transfections were performed in the presence of chloroquine to evaluate the contribution of lysosomal degradation of pDNA:protein complexes. Cells were pre-incubated for 4 h with chloroquine (100 μM) (Sigma–Aldrich). For these assays, pre-treated cells were incubated in the presence of different complexes for 4 h, after which the medium was replaced with fresh growth medium. After 24 h, cells were collected, and the luciferase activity was measured as described above. The experiments were performed as three independent replicates and the results were normalized as percentages, and the value of luciferase expression (in RLU/mg) of the control was defined as 100%.

2.7. In vitro toxicity

Cytotoxicity of the delivery vectors was assessed using the Cell Proliferation Reagent WST-1 (Roche Applied Science) following the manufacturer's instructions. Briefly, HeLa cells were grown in 96-well plates to 70% confluence and then transfected as described above with pDNA:protamine (pDNA:protein molar ratio of 1:8000) or pDNA:T-Rp3 (pDNA:protein molar ratio of 1:8000) complexes with and without Lipofectamine 2000™; pDNA alone served as the control. The experiments were performed as six independent replicates. The complexes were prepared as previously described (item 2.5) using a final volume (20 μL) proportional to the 96 wells. The mass of pDNA used per well was 0.2 μg and all pDNA:protein molar rations were kept the same. Lipofection using Lipofectamine 2000™ was carried out using 0.2 μg pDNA plus 0.3 μL reagent in 20 μL of medium per well. The cells were exposed to the complexes for 6 h, when the medium was replaced. The plates were analyzed 24 h post-transfection. Analysis was done by adding 10 μL of WST-1 reagent to each well, followed by incubation for an additional hour. Absorbance was recorded at 440 nm in an ELISA reader.

2.8. Cellular uptake

Cellular uptake and trafficking of vectors were examined using a Zeiss LSM780-NLO laser scanning confocal microscope with a Plan-Apochromat 63× oil objective (NA 1.45). Plasmids pVAX1-LUC were covalently labeled with Cy3™ (Label IT, Mirus) and used for HeLa cell transfection as previously described. Cells were collected at different time points (6, 12 and 24 h post-transfection), rinsed with PBS, fixed (formaldehyde 3.7% in PBS for 5 min), permeabilized and blocked. For microtubule staining, cells were incubated with anti-α-tubulin overnight followed by incubation with Alexa Fluor™ 488-coupled secondary antibody (both from Molecular Probes-Invitrogen) for 2 h. After washing in PBS, cells were stained with 4,6-diamino-2-phenylindole (DAPI), washed again and kept in PBS. The 3D image measurements through the depth of the cell were reconstructed and deconvoluted using AutoQuantX2 (Media Cybernetics Inc., USA). All deconvoluted image stacks were further reconstructed by voxel-based volume and isosurface rendering using Imaris (Bitplane) to determine the localization of the vector particles within the cells.

2.9. Time-lapse microscopy

Time-lapse imaging assays were performed on live HeLa cells (phase) transfected with pDNA:T-Rp3 complexes (Cy3-labeled pDNA, in red). HeLa cells were seeded on a sterile 35-mm glass bottom dish (Hi-Q4 culture dish) and grown to 40% confluence. The medium was then replaced by a fresh medium containing the labeled complexes and the culture dish was placed into the live-imaging chamber of a Nikon BioStation IM-Q (Nikon). Multiple image capture points were selected and captured for 11 h using 20× magnification. Time-lapse microscopy was also performed in the presence of chloroquine.

2.10. Statistics

Statistical significance of the transfection results (transfection level, effect of drugs and cytotoxicity) was determined using the two-tailed Student's *t*-test, assuming unequal variances, at a significance level $p < 0.05$. The data were presented as the mean ± standard deviation. The number of independent experiments in each analysis is presented in Section 2. Analyses were performed using the Microsoft Excel Data Analysis ToolPack 2007 (Microsoft).

3. Results and discussion

3.1. T-Rp3 fusion protein expression in E. coli

During the design of a novel modular protein, special care should be taken to avoid steric hindrance of the functional domains or sequences. We have recently reported the cloning, purification and structural characterization of human Rp3 to determine its potential use as a gene carrier (Toledo et al., 2013). Here, the cloning of a new protein (T-Rp3) was performed with the insertion of a TAT sequence at the C-terminus of the Rp3 protein, in addition to the fusion of the histidine tail and the DNA-binding domain to the N-terminus (Fig. 1). This construction was chosen to prevent the blockage of domains involved in the interaction with the dynein motor complex, based on the available structural data for TcTex (Williams, 2005) and dynein complex formation data (Barbar et al., 2001). We also took into consideration a low-resolution structural model generated by SAXS for the recombinant Rp3 (Toledo et al., 2013). The short TAT sequence (11 amino acid residues) was fused to the C-terminus of the Rp3 protein to increase the probability of this membrane active sequence to be exposed following complex formation with pDNA.

3.2. T-Rp3 interaction in vitro with dynein intermediate chain

After the successful expression and purification of T-Rp3 (Supplementary data, Fig. 1S), we evaluated whether the recombinant protein retained the ability to interact with the dynein intermediate chain *in vitro*. Since C-terminal region of T-Rp3 contains TAT peptide and is probably involved in light chain dimerization and interaction with the dynein complex (Makokha et al., 2002), we analyzed the interaction of recombinant T-Rp3 with human dynein intermediate chain DYNIC2 (isoform C) *in vitro*. The results of the affinity chromatography assay indicated a strong interaction between T-Rp3 and the immobilized intermediate chain, as shown in the SDS-PAGE gel prepared with the fractions collected during the chromatography steps (Fig. 2A). The T-Rp3 could only be eluted from the column containing the immobilized intermediate chain under strongly acidic conditions (pH 3.0). Additionally, this interaction could not be disrupted by a salt gradient, which also pointed to a specific interaction between the recombinant light chains and the immobilized intermediate chain. As a control, we performed

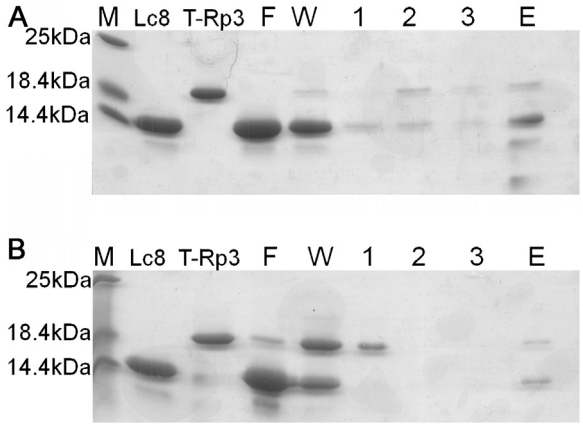

Fig. 2. T-Rp3 interacts with the dynein intermediate chain. The T-Rp3 interaction with the dynein intermediate chain was evaluated in the presence of Lc8 by affinity chromatography in immobilized intermediate chain Sepharose resin. The fractions collected were analyzed in a SDS-PAGE gel. The lanes labeled T-Rp3 and Lc8 represent the proteins alone, before preparation of the equimolar solution. We observed a much stronger interaction in the resin with the immobilized intermediate chain (A) than with the control resin (B). After flow-through (lane F) and washing (lane W), three additional washing steps were performed with an increasing salt gradient (lanes 1–3), and a final step using a pH 3.0 elution buffer (lane E).

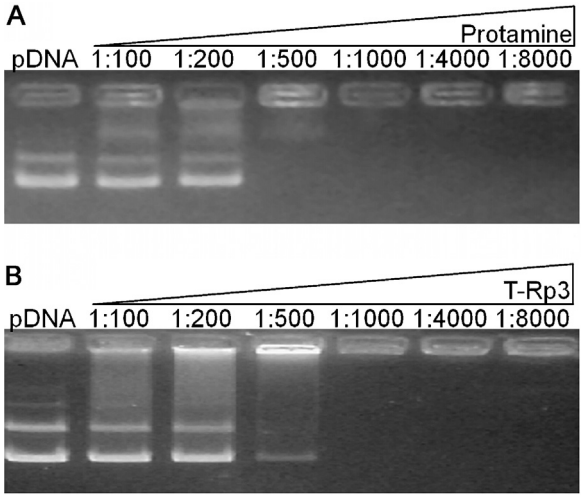

Fig. 3. T-Rp3 interacts with and condenses pDNA. The ability of protamine (A) and T-Rp3 (B) to interact with and to condense plasmid DNA was analyzed by gel retardation assays. Six pDNA:protein molar ratios were studied, as shown in the gel captions.

the chromatography using a resin without the intermediate chain (CNBr-activated Sepharose blocked with Tris) and observed only nonspecific interaction, with most of the T-Rp3 being eluted during the flow-through, washing and salt gradient steps (Fig. 2B). Taken together, these are strong indications that the recombinant T-Rp3 retains the ability to interact with the dynein intermediate chain *in vitro*.

3.3. T-Rp3 interaction with plasmid DNA

Gel retardation assays (Fig. 3) demonstrate that the interaction of T-Rp3 with pDNA is molar ratio dependent, with similar results to protamine, an arginine-rich protein important in spermatogenesis, responsible for inducing torus formation and DNA packaging (Brewer, 1999). This effect can be attributed to the addition of DNA-binding and TAT domains, as both are positively charged. In agreement with this observation, wild-type Rp3 (without DNA-binding or TAT) exhibits no significant capacity to interact with

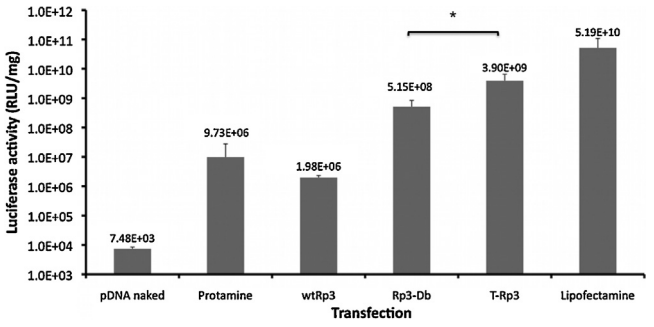

Fig. 4. Compared efficiency of T-Rp3. Transfection efficiency of HeLa cells comparing naked pDNA, protamine, wild-type Rp3 (Rp3), Rp3 containing the synthetic DNA-binding sequence (Rp3-Db), T-Rp3 (containing the DNA-binding and TAT sequences), and Lipofectamine 2000™. The molar ratio used for all pDNA:protein complexes was 1:8000. Transfection efficiency was assessed by measuring the activity of the luciferase reporter enzyme. Error bars indicate the standard deviation of replicates (See Section 2). The signal (*) indicates that the results are significantly different ($p < 0.05$) when compared between the pairs. The *y*-axis is presented using a $\log_{10}$ scale.

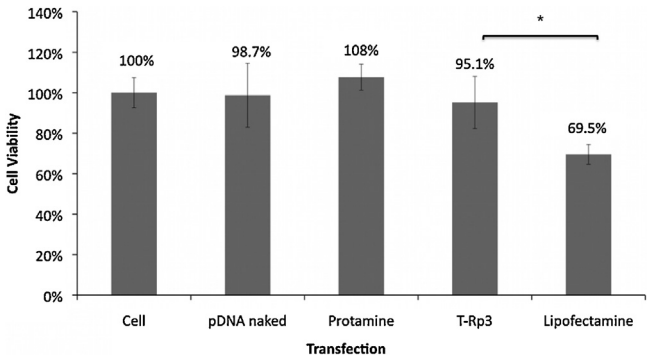

Fig. 5. Evaluation of the cytotoxicity of different delivery vectors for HeLa cells. The assays were performed using the WST-1 reagent (Roche Applied Science). We assayed cell viability following transfection with complexes formed by pDNA and Lipofectamine 2000™, protamine and T-Rp3 as previously described. Error bars indicate the standard deviation of six replicates performed independently. The signal (*) indicates that the results are significantly different ($p < 0.05$) when compared between the pairs.

pDNA, even at higher molar ratios (data not shown). Analysis of the zeta potential of the pDNA:T-Rp3 particles shows that it has a positive charge (+28.6 mV) at the 1:8000 molar ratio, while the pDNA:protamine net charge was +14.3 mV. Furthermore, dynamic light scattering assays indicate that at a molar ratio of 1:8000, the pDNA:T-Rp3 particles are smaller and more stable when compared to protamine under the same conditions. While pDNA:protamine particle size increased from 213 to 575 nm in 1 h, T-Rp3 formed smaller particles (77 nm) that did not increase much in size (95 nm) after the same period (Supplementary data, Fig. 2S).

3.4. Evaluation of T-Rp3 mediated gene delivery in cultured HeLa cells

The efficiency of pDNA delivery mediated by T-Rp3 in cultured HeLa cells was evaluated and compared to the efficiency of the wild-type Rp3 (wtRp3) and a T-Rp3 construct lacking the TAT sequence (Rp3-Db), as well as protamine. As observed in Fig. 4, wtRp3 presented a significant but limited efficiency to deliver pDNA. This can be explained by the low theoretical isoelectric point of wtRp3 (p*I* of 6.0), which results in a weak electrostatic interaction with pDNA, as verified by the gel retardation assay (data not shown). The insertion of the N-terminus synthetic DNA-binding (Rp3-Db) increased luciferase expression by 260 times. However, the addition of the TAT and DNA-binding sequences to Rp3 (T-Rp3) was associated with an approximately 2000-fold increase in luciferase expression. In fact, the transfection efficiencies of T-Rp3 and Rp3-Db were not much different as initially expected. However, although these two proteins have not been compared under every aspect, the addition of the TAT domain to Rp3-Db (T-Rp3) still increased the vector efficiency by 7.6-fold ($p < 0.05$). Moreover, T-Rp3 is more stable and allows easier manipulation during protein purification steps, probably as a result of the higher p*I* and reduced propensity to electrostatic aggregation (data not shown).

Compared to protamine, T-Rp3 presented a 400-fold increase in transgene expression, and a 13-fold increase was found in comparison to the previously reported LD4, the LC8 based recombinant protein (Toledo et al., 2012). The molar ratios used were chosen based on our previous experience (Toledo et al., 2012) and from preliminary studies comparing the transfection efficiency of protamine and T-Rp3 at different molar ratios (data not shown). The 1:8000 pDNA:protein molar ratio was found to be the best, similarly to our previous results with LD4 (Toledo et al., 2012). High molar ratios are necessary to form particles with high zeta potential values, which may contribute to a reduced propensity to aggregate and to promote high transfection efficiencies. Furthermore, in the case of T-Rp3, the increase in the number of TAT sequences on the surface of the cargos (complexes) may also increase their efficiency of escape from endosomes/lysosomes during intracellular trafficking (Erazo-Oliveras et al., 2012).

In addition, we compared the transfection efficiency of T-Rp3 to Lipofectamine 2000™, a cationic lipid that is highly efficient *in vitro*. The pDNA delivery mediated by Lipofectamine 2000™ resulted in a luciferase expression 13 times higher than that found for T-Rp3 (Fig. 4). Lipofectamine 2000™ is known to improve endosomal escape and delivery to the cytosol, including a fast nuclear translocation capability (Akita et al., 2004). For a better evaluation of the T-Rp3 efficiency, we performed transfections using the pVAX1-GFP plasmid, which differs from pVAX1-Luc by the presence of a *GFP* reporter gene instead of *luciferase* (Azzoni et al., 2007). Flow cytometry analysis of the HeLa cells transfected by the pDNA:T-Rp3 complexes resulted in a value of 14% of positive cells, while the value found for Lipofectamine 2000™ was 23%.

3.5. Evaluation of cytotoxicity

Transfection efficiency is not the only important characteristic of a non-viral vector designed for *in vivo* studies. Vectors should also be of low cytotoxicity and immunogenicity. An advantage of T-Rp3 is that most of its amino acid sequence is composed by the human dynein light chain Rp3, which is endogenously expressed in human cells (King, 2000). In a comparative study of efficiency and toxicity of four different protein transduction domains, the TAT sequence was found to be of low cytotoxicity to HeLa cells (Sugita et al., 2009). We also performed an evaluation of the *in vitro* toxicity of T-Rp3, protamine and Lipofectamine 2000™ by measuring the activity of mitochondrial dehydrogenase (Fig. 5). Protamine and T-Rp3 had a reduced toxic effect and, as expected, Lipofectamine 2000™ had the highest cytotoxicity for HeLa cells, with a decrease in cell viability of approximately 30%. The cytotoxic effects of cationic lipids and especially Lipofectamine 2000™ have been reported by others (Spagnou et al., 2004; Zhang et al., 2007).

3.6. Microtubule involvement and endosomal escape

As discussed above, among the desired features of pDNA:T-Rp3 particles have the ability to interact with the microtubule network for fast intracellular trafficking and an improved endosomal escape capability. To evaluate the dependence of these particles on the microtubules, we performed transfections in the presence of

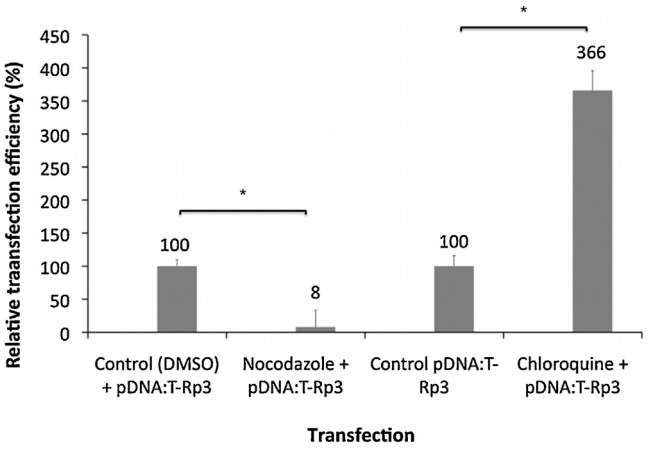

Fig. 6. Involvement of microtubules and endosomes in the transfection efficiency of HeLa cells using T-Rp3:pDNA complexes at a 1:8000 pDNA:T-Rp3 molar ratio. The involvement of microtubules was studied using nocodazole. Chloroquine was used to investigate the effect of the endosomal/lysosomal entrapment as a barrier to gene delivery. Error bars indicate the standard deviation of triplicate measurements performed independently. The signal (*) indicates that the results are significantly different ($p < 0.05$) when compared between the pairs.

nocodazole, a microtubule-depolymerizing agent that is expected to decrease the delivery efficiency of T-Rp3. In fact, in the presence of this drug, luciferase expression was reduced by 92%, suggesting that T-Rp3 is highly dependent on microtubules for pDNA delivery (Fig. 6). This is an interesting result and an indication that microtubules are involved in the transport of T-Rp3 complexes. For comparison, transfections performed with protamine and Lipofectamine 2000™ exhibited much smaller decrease in luciferase expression in the presence of nocodazole (56% and 41%, respectively). However, these results were not statistically significant at a significance level of $\alpha = 0.05$ (data not shown). Although this is not a proof of direct and specific interaction with dyneins, these results indicate that pDNA:T-Rp3 complexes strongly rely on active transport along microtubules to reach the nucleus.

Additionally, we assessed the level of entrapment of pDNA:T-Rp3 particles inside endosomes and lysosomes, which is another major limiting step in efficient gene delivery. Transfections were performed in the presence of chloroquine, a weak base that is often used to investigate endosomal entrapment. Chloroquine accumulates in acidic organelles such as late endosomes and lysosomes, raising the luminal pH of the organelles and preventing enzymatic degradation of non-viral vectors. Under the conditions tested, we observed that chloroquine promoted an approximately 4-fold increase in the reporter enzyme expression (Fig. 6). This finding indicates that endosomal entrapment remains an important limiting factor despite the presence of an N-terminal histidine tail and a C-terminal TAT sequence. Although it is reported that TAT-delivered cargos frequently remain trapped inside endocytic organelles (Brooks et al., 2005; Erazo-Oliveras et al., 2012), the presence of histidine residues (six in T-Rp3) tends to induce a proton sponge effect in such organelles, which increases their osmolarity, promotes swelling and, ultimately, lysis. For this reason, during the design of a gene vehicle, we should also take in consideration that an excessive increase in endo/lysosomal escape capability can result in higher cytotoxic effects due to vesicle disruptions and the release of pro-apoptotic and cytotoxic proteases.

3.7. Investigation of cellular uptake using confocal microscopy

Generally, the internalization of plasmid DNA particles mediated by TAT or arginine-rich peptides (such as the synthetic DNA-binding sequence in T-Rp3) occurs by endocytosis, mostly *via* the clathrin-dependent pathway, although a multiplicity of different entry pathways also tends to occur in parallel (Brooks et al., 2005). Here, we visualized the cellular uptake of pDNA:T-Rp3

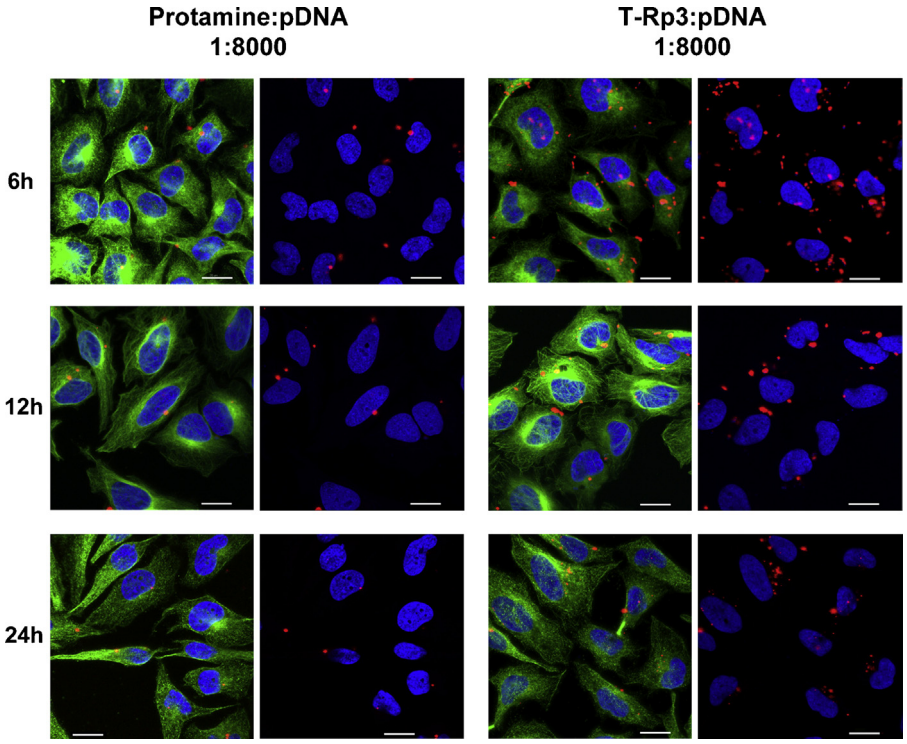

Fig. 7. Intracellular distribution of Cy3-labeled plasmid DNA in transfected HeLa cells. Transfections were mediated by protamine or T-Rp3 and images were collected at different time points by laser scanning confocal microscopy. Plasmid DNA can be seen in red (Cy3), microtubules are shown in green (Alexa Fluor 488), and the nuclei in blue (Dapi). Scale bars represent 20 μm. (For interpretation of the references to color in this figure legend, the reader is referred to the web version of the article.)

and pDNA:protamine complexes by HeLa cells at three different time points (6, 12 and 24 h post-transfection) (Fig. 7). The first difference observed was that, after washing and fixing, a higher amount of pDNA was internalized by cells transfected using T-Rp3, confirming the higher efficiency indicated by the luciferase expression results (Fig. 5). The pDNA distribution pattern, mainly in large and well-defined spots, is consistent with internalization by endocytosis and entrapment inside vesicles that tend to reduce in number overtime. This observation is also consistent with the results of the transfections performed in the presence of chloroquine (Fig. 6). However, despite the risk of artifacts due to fixation procedures, a difference in distribution pattern can be observed between the pDNA delivered by T-Rp3 and protamine. Compared to the protamine-mediated delivery, pDNA internalized by T-Rp3 is frequently observed not only inside large vesicles but also as small particles in the cytosol, indicating differences in the cellular uptake pathway and/or improved endosomal escape capability. This result is consistent with our data indicating that transfection efficiency mediated by protamine increases 10-fold in the presence of chloroquine (Toledo et al., 2012) in comparison with the 4-fold increase observed in T-Rp3 mediated transfections (Fig. 6).

At 6 h post-transfection, pDNA can be observed in the nucleus. This result was expected because a significant level of luciferase activity is detected at this time point (Supplementary data, Fig. 3S). Over time, pDNA red fluorescence is reduced, probably due to the degradation inside endosomal/lysosomal vesicles, as indicated by the presence of large red vesicles observed at 12 h post-transfection. Interestingly, differently from protamine, a significant amount of pDNA can be observed in the cells 24 h after T-Rp3 mediated transfection. Additionally, the vectors (Cy3-labeled pDNA, seen in red) are frequently concentrated at the perinuclear region of the cells, tending to co-localize with a dense concentration of microtubules (probably centrosomes), as can be observed in Figs. 8 and 4S. In contrast, protamine-mediated transfection frequently leads to cells containing only one or two large red spots, probably formed by pDNA trapped inside vesicles, and usually not co-localizing with dense microtubule concentrations (Fig. 7). The significant differences in cell uptake between T-Rp3 and protamine-mediated transfection were also captured by time-lapse live cell imaging (Videos 1 and 2, Supplementary data).

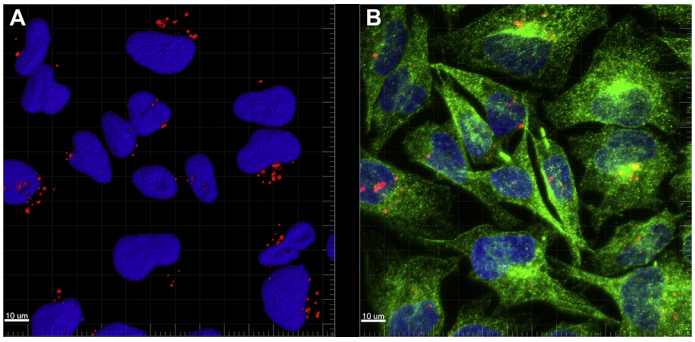

Fig. 8. Three dimensional distribution of Cy3-labeled pDNA (red) in HeLa cells transfected with pDNA:T-Rp3 complexes (A), indicating the presence of pDNA at the proximity of the nuclei (blue). Images were taken 24 h post-transfection using a laser scanning confocal microscope and were deconvoluted during post-processing. (B) Microtubules are stained in green (Alexa Fluor 488) and pDNA tends to co-localize with a dense concentration of microtubules. (For interpretation of the references to color in this figure legend, the reader is referred to the web version of the article.)

The images of intracellular trafficking of Lipofectamine 2000™-mediated transfections are not presented here, due to the distinct nature of this cationic lipid in comparison to protein vectors, and to the fact that it has been the subject of previous studies (Akita et al., 2004; Kamiya et al., 2002). Although cellular uptake of pDNA:Lipofectamine complexes occur mainly by endocytosis, escape from endosomal/lysosomal vesicles and nuclear translocation is faster and more efficient than peptide-mediated transfections, which is consistent with the high transfection efficiency of this lipid (Akita et al., 2004).

Time-lapse microscopy of the transfected cells in the presence of chloroquine indicated that perinuclear localization of the complex is fast (within less than 1 h), occurring during the period necessary for the setting of the live image equipment (Fig. 9). The pDNA:T-Rp3 complexes tended to accumulate in the perinuclear region of the cells even in the presence of chloroquine. This observation suggests

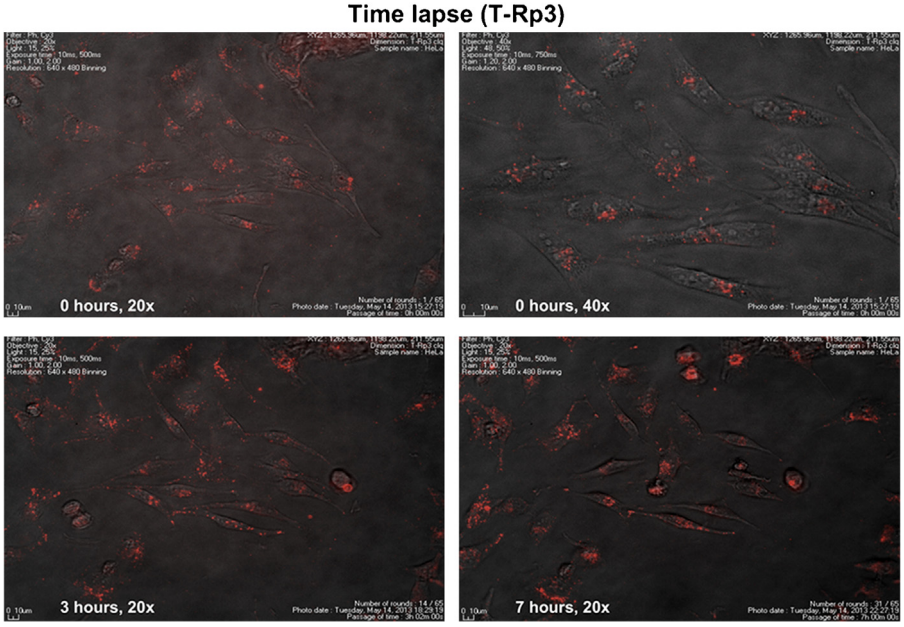

Fig. 9. Sequences of photographs taken from time-lapse imaging experiment at three different times after the transfection of HeLa cells (phase) with pDNA:T-Rp3 complexes (Cy3-labeled pDNA in red) and in the presence of chloroquine. The images taken at "0 h" (corresponding to approximately 1 h post-transfection, due to the time necessary to set the equipment) show a high level of complex internalization. The images also indicate that pDNA tends to accumulate at the proximity of the nuclei even in the presence of chloroquine. (For interpretation of the references to color in this figure legend, the reader is referred to the web version of the article.)

that active transport of the complexes occurs as a result of not only the movement of endocytic vesicles toward lysosomes but also the interaction of free pDNA:T-Rp3 complexes with microtubules.

4. Conclusion

We designed the recombinant protein T-Rp3 as a modular protein with the intention to mimic viral vectors that take advantage of the microtubules for a faster intracellular movement toward the nucleus. The protein proved to efficiently interact with and to condense pDNA, forming small positively charged particles. These are regarded as crucial features for effective non-viral gene delivery vectors and may contribute to the T-Rp3 performance during transfection. Transfection assays using HeLa cells showed that T-Rp3 is a very efficient delivery vehicle, even when compared with Lipofectamine 2000™, presenting a reduced cytotoxicity. The confocal microscopy studies indicated fast perinuclear accumulation of pDNA following transfection, co-localizing with dense concentrations of microtubules. The results presented here strongly indicate that the cell microtubule network plays an important role in the trafficking of pDNA:T-Rp3 particles. However, due to the complex nature of these vectors and the diversity of cellular entry pathways and intracellular trafficking, investigating the pDNA:T-Rp3 routes inside the cells is a very challenging tasks. Vectors may rely on the microtubule network by different forms, including direct or indirect interaction and also transport inside endocytic vesicles. These different intracellular routes may also happen as parallel events. The detailed understanding of the mechanisms involved in the intracellular trafficking of modular protein vectors is one of the major goals of our group and the studies are still in progress. Taken together, the results presented here indicate that the strategy of exploiting dynein light chains for the design of modular recombinant proteins is promising and may significantly contribute to the development of more efficient non-viral gene delivery vectors.

Acknowledgments

The authors gratefully acknowledge the financial support of the Fundação de Amparo à Pesquisa do Estado de São Paulo – FAPESP (São Paulo, Brazil, Grant 2007/58323-9) and Conselho Nacional de Desenvolvimento Científico e Tecnológico – CNPq (Brazil, Grant 471971/2011-1). We also thank the Laboratório de Espectroscopia e Calorimetria (LEC), Laboratório Nacional de Biociências – LNBio (Campinas, Brazil), and the National Institute of Science and Technology on Photonics Applied to Cell Biology (INFABIC), UNICAMP, for the support for the analysis of recombinant T-Rp3. Finally, we thank Professor Maricilda Palandi de Mello, CBMEG, UNICAMP (Campinas, Brazil), for support for the HeLa cell culture.

Appendix A. Supplementary data

Supplementary data associated with this article can be found, in the online version, at http://dx.doi.org/10.1016/j.jbiotec.2014.01.001.

References

Akita, H., Ito, R., Khalil, I.A., Futaki, S., Harashima, H., 2004. Quantitative three-dimensional analysis of the intracellular trafficking of plasmid DNA transfected by a nonviral gene delivery system using confocal laser scanning microscopy. Mol. Ther. 9, 443–451.

Azzoni, A.R., Ribeiro, S.C., Monteiro, G.A., Prazeres, D.M.F., 2007. The impact of polyadenylation signals on plasmid nuclease-resistance and transgene expression. J. Gene Med. 9, 392–402.

Barbar, E., Kleinman, B., Imhoff, D., Li, M., Hays, T.S., Hare, M., 2001. Dimerization and folding of LC8, a highly conserved light chain of cytoplasmic dynein. Biochemistry 40, 1596–1605.

Brewer, L.R., 1999. Protamine-induced condensation and decondensation of the same DNA molecule. Science 286, 120–123.

Brooks, H., Lebleu, B., Vives, E., 2005. Tat peptide-mediated cellular delivery: back to basics. Adv. Drug Deliv. Rev. 57, 559–577.

Dodding, M.P., Way, M., 2011. Coupling viruses to dynein and kinesin-1. EMBO J. 30, 3527–3539.

Douglas, M.W., 2004. Herpes simplex virus type 1 capsid protein VP26 interacts with dynein light chains RP3 and Tctex1 and plays a role in retrograde cellular transport. J. Biol. Chem. 279, 28522–28530.

Döhner, K., Nagel, C.-H., Sodeik, B., 2005. Viral stop-and-go along microtubules: taking a ride with dynein and kinesins. Trends Microbiol. 13, 320–327.

Edelstein, M.L., Abedi, M.R., Wixon, J., 2007. Gene therapy clinical trials worldwide to 2007 – an update. J. Gene Med. 9, 833–842.

Erazo-Oliveras, A., Muthukrishnan, N., Baker, R., Wang, T.-Y., Pellois, J.-P., 2012. Improving the endosomal escape of cell-penetrating peptides and their cargos: strategies and challenges. Pharmaceuticals 5, 1177–1209.

Ferrer-Miralles, N., Vázquez, E., Villaverde, A., 2008. Membrane-active peptides for non-viral gene therapy: making the safest easier. Trends Biotechnol. 26, 267–275.

Freitas, S.S., Azzoni, A.R., Santos, J.A.L., Monteiro, G.A., Prazeres, D.M.F., 2007. On the stability of plasmid DNA vectors during cell culture and purification. Mol. Biotechnol. 36, 151–158.

Ganta, S., Devalapally, H., Shahiwala, A., Amiji, M., 2008. A review of stimuli-responsive nanocarriers for drug and gene delivery. J. Control. Release 126, 187–204.

Gump, J.M., Dowdy, S.F., 2007. TAT transduction: the molecular mechanism and therapeutic prospects. Trends Mol. Med. 13, 443–448.

Hall, J., Karplus, P.A., Barbar, E., 2009. Multivalency in the assembly of intrinsically disordered dynein intermediate chain. J. Biol. Chem. 284, 33115–33121.

Holzbaur, E.L., Vallee, R.B., 1994. Dyneins: molecular structure and cellular function. Annu. Rev. Cell Biol. 10, 339–372.

Kamiya, H., Fujimura, Y., Matsuoka, I., Harashima, H., 2002. Visualization of intracellular trafficking of exogenous DNA delivered by cationic liposomes. Biochem. Biophys. Res. Commun. 298, 591–597.

Kay, M.A., 2011. State-of-the-art gene-based therapies: the road ahead. Nat. Rev. Genet. 12, 316–328.

King, S.M., 2000. The dynein microtubule motor. Biochim. Biophys. Acta 1496, 1–16.

Lo, K.W.H., 2004. The 8-kDa dynein light chain binds to p53-binding protein 1 and mediates DNA damage-induced p53 nuclear accumulation. J. Biol. Chem. 280, 8172–8179.

Lukacs, G.L., Haggie, P., Seksek, O., Lechardeur, D., Freedman, N., Verkman, A.S., 2000. Size-dependent DNA mobility in cytoplasm and nucleus. J. Biol. Chem. 275, 1625–1629.

Lv, H., Zhang, S., Wang, B., Cui, S., Yan, J., 2006. Toxicity of cationic lipids and cationic polymers in gene delivery. J. Control. Release 114, 100–109.

Makokha, M., Hare, M., Li, M., Hays, T., Barbar, E., 2002. Interactions of cytoplasmic dynein light chains Tctex-1 and LC8 with the intermediate chain IC74. Biochemistry 41, 4302–4311.

Mastrobattista, E., van der Aa, M.A.E.M., Hennink, W.E., Crommelin, D.J.A., 2006. Artificial viruses: a nanotechnological approach to gene delivery. Nat. Rev. Drug Discov. 5, 115–121.

Medina-Kauwe, L.K., Xie, J., Hamm-Alvarez, S., 2005. Intracellular trafficking of non-viral vectors. Gene Ther. 12, 1734–1751.

Mesika, A., Kiss, V., Brumfeld, V., Ghosh, G., Reich, Z., 2005. Enhanced intracellular mobility and nuclear accumulation of DNA plasmids associated with a karyophilic protein. Hum. Gene Ther. 16, 200–208.

Moschos, S.A., Jones, S.W., Perry, M.M., Williams, A.E., Erjefalt, J.S., Turner, J.J., Barnes, P.J., Sproat, B.S., Gait, M.J., Lindsay, M.A., 2007. Lung delivery studies using siRNA conjugated to TAT(48–60) and penetratin reveal peptide induced reduction in gene expression and induction of innate immunity. Bioconjug. Chem. 18, 1450–1459.

Moseley, G.W., Leyton, D.L., Glover, D.J., Filmer, R.P., Jans, D.A., 2010. Enhancement of protein transduction-mediated nuclear delivery by interaction with dynein/microtubules. J. Biotechnol. 145, 222–225.

Nitin, N., LaConte, L., Rhee, W.J., Bao, G., 2009. Tat peptide is capable of importing large nanoparticles across nuclear membrane in digitonin permeabilized cells. Ann. Biomed. Eng. 37, 2018–2027.

Ruponen, M., Arkko, S., Urtti, A., Reinisalo, M., Ranta, V.-P., 2009. Intracellular DNA release and elimination correlate poorly with transgene expression after non-viral transfection. J. Control. Release, 1–6.

Said Hassane, F., Saleh, A.F., Abes, R., Gait, M.J., Lebleu, B., 2009. Cell penetrating peptides: overview and applications to the delivery of oligonucleotides. Cell. Mol. Life Sci. 67, 715–726.

Spagnou, S., Miller, A.D., Keller, M., 2004. Lipidic carriers of siRNA: differences in the formulation, cellular uptake, and delivery with plasmid DNA. Biochemistry 43, 13348–13356.

Sugita, T., Yoshikawa, T., Mukai, Y., Yamanada, N., Imai, S., Nagano, K., Yoshida, Y., Shibata, H., Yoshioka, Y., Nakagawa, S., Kamada, H., Tsunoda, S.-I., Tsutsumi, Y., 2009. Comparative study on transduction and toxicity of protein transduction domains. Br. J. Pharmacol. 153, 1143–1152.

Suh, J.J., Wirtz, D.D., Hanes, J.J., 2003. Efficient active transport of gene nanocarriers to the cell nucleus. Proc. Natl. Acad. Sci. U.S.A. 100, 3878–3882.

Toledo, M.A.S., Favaro, M.T.P., Alves, R.F., Santos, C.A., Beloti, L.L., Crucello, A., Santiago, A.S., Mendes, J.S., Horta, M.A.C., Aparicio, R., Souza, A.P., Azzoni, A.R., 2013. Characterization of the human dynein light chain Rp3 and its use as a

non-viral gene delivery vector. Appl. Microbiol. Biotechnol., http://dx.doi.org/10.1007/s00253-013-5239-5.
Toledo, M.A.S., Janissen, R., Favaro, M.T.P., Cotta, M.A., Monteiro, G.A., Prazeres, D.M.F., Souza, A.P., Azzoni, A.R., 2012. Development of a recombinant fusion protein based on the dynein light chain LC8 for non-viral gene delivery. J. Control. Release 159, 222–231.
Tzfira, T., 2006. On tracks and locomotives: the long route of DNA to the nucleus. Trends Microbiol. 14, 61–63.
Vázquez, E., Ferrer-Miralles, N., Villaverde, A., 2008. Peptide-assisted traffic engineering for nonviral gene therapy. Drug Discov. Today 13, 1067–1074.
Williams, J.C., 2005. Crystal structure of dynein light chain TcTex-1. J. Biol. Chem. 280, 21981–21986.
Won, Y.-W., Lim, K.S., Kim, Y.-H., 2011. Intracellular organelle-targeted non-viral gene delivery systems. J. Control. Release, 1–11.
Yamano, S., Dai, J., Yuvienco, C., Khapli, S., Moursi, A.M., Montclare, J.K., 2011. Modified Tat peptide with cationic lipids enhances gene transfection efficiency via temperature-dependent and caveolae-mediated endocytosis. J. Control. Release 152, 278–285.
Zhang, S., Zhao, B., Jiang, H., Wang, B., Ma, B., 2007. Cationic lipids and polymers mediated vectors for delivery of siRNA. J. Control. Release 123, 1–10.